Enhancing the Mechanical Properties of Alkali-Activated Mortar with Graphene Quantum Dots

Nitikron Weingyod[1,*] Kantipok Hamcumpai[1], Pattharaphon Chindasiriphan[1], Pitcha Jongvivatsakul[1,3] and Suched Likitlersuang[2,3]

[1] *Center of Excellence in Innovative Construction Materials, Department of Civil Engineering, Faculty of Engineering, Chulalongkorn University, Bangkok, 10330, Thailand.*

[2] *Centre of Excellence in Geotechnical and Geoenvironmental Engineering, Department of Civil Engineering, Faculty of Engineering, Chulalongkorn University, Bangkok 10330, Thailand.*

[3] *GreenTech Nexus: Research Center for Sustainable Construction Innovation, Faculty of Engineering, Chulalongkorn University, Bangkok, 10330, Thailand.*

**Corresponding author; E-mail address: 6670136021@student.chula.ac.th*

Abstract

Graphene quantum dots (GQDs) are nanoscale carbon particles with exceptional properties, making them highly suitable for a wide range of applications. In this study, GQDs were incorporated into alkali-activated mortar (AAM) to enhance their workability and mechanical performance. The GQDs were added at dosages of 0.3%, 0.6%, 0.9%, and 1.2% by weight of fly ash. The study investigates the impact of GQDs on key properties of AAM, including compressive strength, flexural strength, porosity, environmental impact, and eco-strength efficiency. The results showed that the addition of 0.3% GQDs significantly improved mechanical strength, with a 39.1% increase in compressive strength compared to the control mixture without GQDs. The flexural strength increased by 38.8% compared to the control mix, while the porosity decreased by 4%. However, when the GQD content exceeded 0.3%, a reductions in both compressive strength and flexural strength was observed. Environmental impact analysis revealed that higher GQD content led to a reduction in carbon emissions. Additionally, the eco-strength efficiency assessment demonstrated that the mix containing 0.3% GQDs achieved the highest eco-strength efficiency among all tested mixes. This finding underscores the potential of GQD-enhanced AAM for practical, sustainable applications.

Keywords: Alkali-activated material, Carbon emission, Environmental impact, Fly ash, Graphene quantum dots (GQDs)

1. Introduction

In recent years, the greenhouse effect became a significant driver of extreme climate events, including droughts and rising average temperatures [1]. Cement production, accounting for approximately 7% of global CO_2 emissions, was one of the major contributors to anthropogenic emissions, underscoring the urgent need for sustainable alternatives within the construction industry, such as the transition to low-carbon binder materials like alkali-activated materials (AAMs) and geopolymers. [2, 3].

The synthesis of AAMs involves the use of an aluminosilicate precursor, which reacts with an alkali activator, initiating a polymerization reaction [4]. This process results in AAM pastes with properties similar to those of cement paste. The aluminosilicate precursors are typically sourced from industrial solid wastes, including slag, fly ash, and other aluminosilicate materials [5]. These industrial by-products contribute to environmental pollution and disposal challenges, particularly fly ash from coal-fired power plants. Coal combustion contributes to 27% of global energy production and 38% of global electricity generation [6].

AAMs offer a viable alternative to Portland cement, with their binding capacity resulting from the chemical activation of industrial by-products that serve as aluminosilicate sources [7]. Unlike Portland cement-based materials, which primarily produce hydration products such as calcium silicate hydrate (C-S-H), calcium hydroxide, and ettringite, the binding capacity of

AAMs comes from two main gel phases: calcium aluminosilicate hydrate (C-A-S-H) and sodium (or potassium) aluminosilicate hydrate ((N,K)-A-S-H) [8]. Over the past few decades, AAMs have gained recognition as environmentally friendly alternatives to traditional cementitious materials [9]. Moreover, previous studies [10, 11] have demonstrated that AAM production results in lower CO_2 emissions compared to traditional cement production, further reinforcing their potential as an eco-friendly alternative.

Graphene quantum dots (GQDs), characterized by crystal sizes ranging from 5 to 20 nm, were novel carbon-based materials that hold significant potential to revolutionize material engineering [12]. GQDs exhibited exceptional mechanical strength, thermal and electrical conductivity, and hydrophobic properties, owing to their nanoscale dimensions and two-dimensional structure [13]. GQDs have been utilized as additives in cement-based materials to improve their environmental sustainability. The exceptional properties of GQDs make them an effective catalytic material, making them well-suited for use as an additive to enhance material properties. Win et al. [14] investigated the application of GQDs in the development of cement composites. Their results demonstrated enhancements in workability, compressive strength, and flexural strength, primarily attributed to the improved microstructural bridging mechanism, which facilitates the formation of C-S-H products. According to Raj et al. [15], GQDs were applied as an additive to enhance the performance of railway concrete sleepers. Their findings revealed that incorporating 0.3% GQDs significantly improved concrete properties, including workability, mechanical strength, and durability. Moreover, this approach reduced the CO_2 footprint of railway track production by 668 tons per 100 km compared to tracks manufactured using traditional ordinary Portland cement (OPC). However, research on incorporating nanoparticle additives into AAMs to evaluate their effects on workability and strength remains limited. Further investigation is needed to optimize their application and assess their potential in developing more sustainable alternatives for future industrial use.

Therefore, the objective of this manuscript is to investigate the influence of GQDs on the mechanical properties, porosity, and eco-strength efficiency of AAMs, with the aim of developing a sustainable and high-performance construction material aligned with the goals of environmental sustainability and infrastructure innovation.

2. Materials and procedures

2.1 Materials

The materials utilized in this study include high-calcium fly ash (HCF), sodium metasilicate anhydrous (Na_2SiO_3-anhydrous), natural sand, water, and GQDs. The HCF, shown in Fig. 1, was sourced from the Mae Moh Power Plant located in the Mae Moh District, Lampang Province, Thailand. The fly ash was classified as Class C according to ASTM C618 [16], with a loss on ignition (LOI) of 0.15% and a specific gravity of 2.35. The chemical composition is presented in Table 1.

Sodium metasilicate anhydrous (Na_2SiO_3-anhydrous) was used as an alkali activator. It played a key role in dissolving aluminosilicate from the precursor, promoting the formation of a three-dimensional network structure, and enhancing the binding capacity of the AAMs, as illustrated in Fig. 2. The powdered sodium metasilicate anhydrous used in this study contained 51% SiO_2, 46% Na_2O, and 3% H_2O.

Natural sand, shown in Fig. 3, was used as a fine aggregate and conformed to ASTM C33 [17]. It had a specific gravity of 2.66, a fineness modulus of 2.85, and a water absorption rate of 0.58%.

GQDs were synthesized by CrystalLyte Co., Ltd. under patent number WO2024147021A1 for GC86s (liquid GQDs), as shown in Fig. 4. The GQDs were produced via electrochemical reduction of a saturated CO_2-monoethanolamine (MEA) solution. The density of the GQD-containing MEA solution used in this study was 1,050 kg/m³.

Fig. 1 High-calcium fly ash

Fig. 2 Sodium metasilicate anhydrous

Table 1 Chemical composition of fly ash

Chemical composition	HCF (%)
SiO_2	31.5
CaO	26.4
Al_2O_3	15.0
Fe_2O_3	13.8
SO_3	4.99
MgO	2.76
Na_2O	2.27
K_2O	2.12
TiO_2	0.34
P_2O_5	0.268
BaO	0.144
MnO	0.12

Fig. 3 Natural sand

Fig. 4 GQDs

2.2 Mixture proportions

The AAM mix proportions utilized a liquid/ash (L/A) ratio of 0.29. GQDs were introduced at dosages of 0.3%, 0.6%, 0.9%, and 1.2% by binder weight. The detailed mix proportions are presented in the Table 2.

Table 2 Mix proportions of AAM

Mix	HCF (kg/m^3)	Na_2SiO_3 (kg/m^3)	Water (kg/m^3)	Sand (kg/m^3)	GQDs (kg/m^3)
Control	790	79	252	950	-
GQDs0.3	790	79	252	950	2.4
GQDs0.6	790	79	252	950	4.7
GQDs0.9	790	79	252	950	7.1
GQDs1.2	790	79	252	950	9.5

2.3 AAM mixing procedure

The mixing process for the AAM mortar consists of three main steps. In the first step, a dry mixture of HCF, sodium metasilicate anhydrous, and sand were mixed for three minutes. In the second step, water and the additive material (GQDs) were added, and the mixture was blended for three minutes. In the third step, after mixing, the fresh AAM was placed into a mold, wrapped in a plastic sheet, and cured in an oven at 80 °C for 24 hours. Subsequently, the samples are demolded and allowed to cure in ambient air at room temperature until the testing day.

2.4 Experimental investigations

This experimental study examines the incorporation of GQDs into AAM, with a focus on mechanical properties and environmental impact. The workability, mechanical properties, and durability were assessed through evaluations of flowability, compressive strength, flexural strength, and porosity. For the environmental evaluation, the total equivalent CO_2 emissions and eco-strength efficiency were determined. A total of three specimens was used for each test.

2.4.1 Flowability

To assess the workability of AAM, the flowability of the mortar was evaluated according to the ASTM C1437 [18]

2.4.2 Compressive strength

The compressive strength test was conducted in accordance with ASTM C109 [19]. The testing is performed on three 50×50×50 mm^3 cube specimens, cured for 7, 14, 28, and 90 days.

2.4.3 Flexural strength

The flexural strength of mortar was evaluated in accordance with ASTM C348 [20], using three specimens with dimensions of 40 × 40 × 160 mm^3 at 28 days of age.

2.4.4 Porosity

The porosity was determined in accordance with ASTM C642 [21]. The test is conducted on three cube specimens measuring 50×50×50 mm^3, which were cured for 28 days.

2.4.5 Environmental impact

The total equivalent CO_2 emissions are calculated using Eq. (1), and the obtained values were analyzed the eco-strength efficiency (ESE). The environmental impact is assessed based on the ESE, which is calculated using Eq. (2). The equivalent CO_2 emission factors are illustrated in Table 3.

$$\text{Total of equivalent } CO_2 \text{ emission} = \sum_{i=1}^{n}(QM \times EFM) \quad (1)$$

$$\text{ESE} = \frac{\text{Compessive strength}}{\text{Total of equivalent } CO_2 \text{ emission}} \quad (2)$$

where QM is the quantity of material (kg/m^3), EFM is the equivalent CO_2 emission factor of material (kg CO_2-e/kg).

Table 3 Equivalent CO_2 emission factor

Materials	Equivalent CO2 emission factor (kg CO2-e/kg)
HCF	0.0213 [22]
Sodium metasilicate	0.705 [22]
Sand	0.00471 [22]
GQDs	-0.63 [15]
Water	0 [22]

3. Result and discussion

3.1 Workability

Fig. 5 illustrates the flowability of AAM mortar incorporating GQDs. The results indicate that flowability improved with increasing GQD content. The GQDs1.2 mixture demonstrated the highest flowability at 113%, marking a 9% increase compared to the control mixture. This enhancement is likely due to the intrinsic hydrophilic properties of GQDs, which help improve the mortar's workability [12].

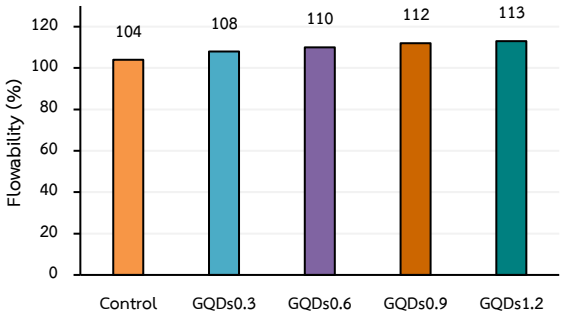

Fig. 5 Flowability of AAM

3.2 Compressive strength

Fig. 6 presents the compressive strength of AAMs incorporating GQDs at curing ages of 7, 14, 28, and 90 days, with values ranging from 16.4 to 33.7 MPa. The results show that adding up to 0.3% GQDs enhanced the compressive strength at all curing ages. The GQDs0.3 mixture exhibited the highest strength at 28 days, reaching 33.4 MPa an increase of 33% compared to the control mixture. This improvement is likely due to the ability of GQDs to accelerate chemical reactions, promoting the formation of C-S-H and C-A-S-H gels, which contribute significantly to strength development [12].

However, when the GQD content exceeded 0.3%, a reduction in compressive strength was observed. This decline may be attributed to the agglomeration of GQDs at higher concentrations, leading to poor dispersion and negatively affecting the composite's performance [23].

Interestingly, the compressive strength at 90 days showed only a marginal increase compared to the 28-day values across all mixtures. This is primarily because the alkali-activation process was nearly complete by 28 days of curing.

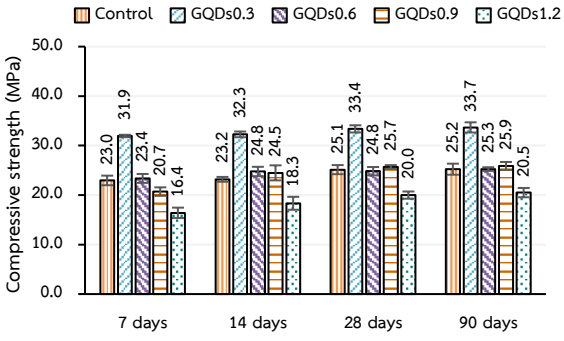

Fig. 6 Compressive strength of AAM

3.3 Flexural strength

The results of the flexural strength test are shown in Fig. 7, with values ranging from 4.8 to 7.4 MPa. The data indicate that flexural strength increased with the addition of GQDs up to 0.3%. However, further increases beyond 0.3% led to a decline in strength. Notably, the GQDs0.3 mixture achieved the highest flexural strength of 7.4 MPa, representing a 40% increase compared to the control mixture. This improvement is likely due to the bridging effect of graphene derivatives, which can function similarly to microfibers, enhancing the flexural performance of the composite [14]. On the other hand, adding more than 0.3% GQDs resulted in reduced flexural strength, following a trend similar to that observed in compressive strength results. This decrease may be attributed to poor dispersion and aggregation of GQDs at higher concentrations, which can negatively affect the composite's integrity.

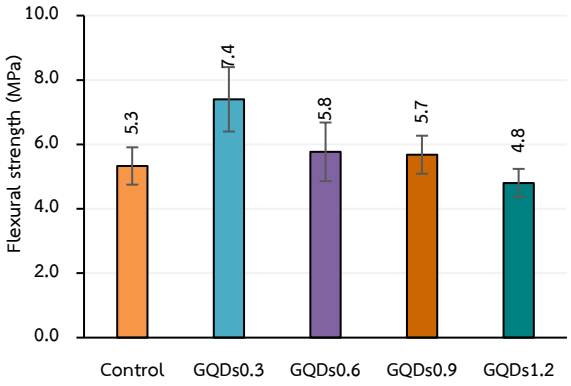

Fig. 7 Flexural strength of AAM

3.4 Porosity

Fig. 8 illustrates the porosity results of AAM incorporating GQDs. Overall, the observed porosity percentage ranged from 15.2% to 19.2%. It discovered that the porosity results were significantly reduced when the GQDs was added in the system. The lowest porosity, 15.2%, was highlighted in GQDs0.3, illustrating a reduction of porosity by 4% compared to control mixture. This is probably due to the enhanced nucleation effect of the graphene derivatives, which facilitates the formation of the C-S-H phase [13]. Previous research has emphasized the capacity of graphene nanomaterials to enhance the refinement of pore distribution [24,25].

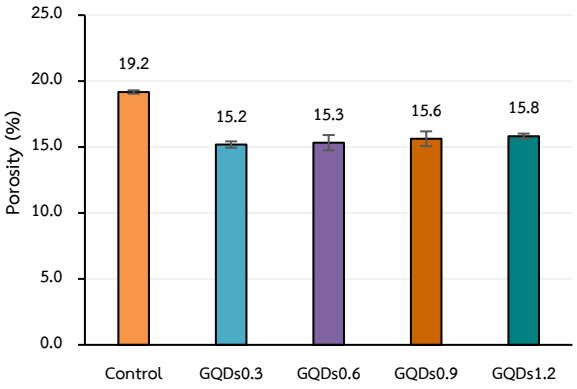

Fig. 8 Porosity of AAM

3.5 Environmental impact

Fig. 9 and Fig. 10 illustrate the total embodied CO_2 emissions and eco-strength efficiency of AAM incorporating GQDs, respectively. Based on the evaluation, it was observed that increasing in GQDs level addition assisted to reduce the embodied CO_2 emissions [26]. During the manufacturing process, CO_2 was utilized in the synthesis of GQDs, thereby classifying them as carbon-negative products. The CO_2 emission factor for GQDs has been reported as -0.63 kg CO_2-equivalents per kilogram [15].

In terms of eco-strength efficiency, the GQDs0.3 mixture exhibited the highest value of 0.467 MPa/kgCO_2 m^3, outperforming all other batches. This obviously indicates a suitable option in both strength and environmental consideration. Consequently, the GQDs0.3 mixture can be considered a suitable candidate for developing eco-friendly construction materials for practical applications.

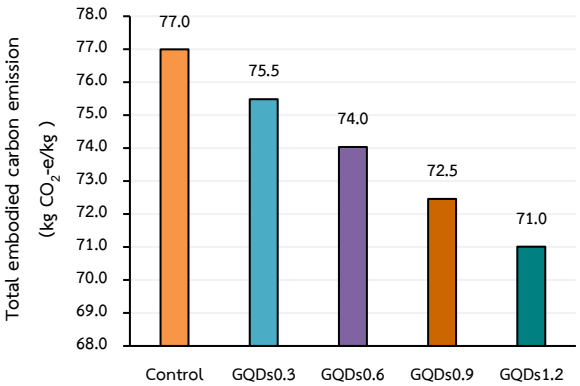

Fig. 9 Total embodied carbon emission of AAM

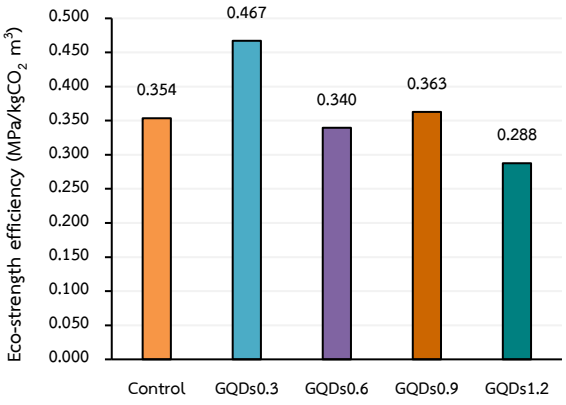

Fig. 10 Eco-strength efficiency of AAM

4. Conclusions

This study explored the incorporation of GQDs in AAM at varying dosages to assess their effects on workability, mechanical properties, durability, and environmental impact. The findings indicate that adding GQDs enhanced flowability, with the highest improvement observed at increased dosages. The optimal performance was observed at a GQD dosage of 0.3%, leading to substantial improvements in mechanical properties and durability. The compressive and flexural strengths at 28 days increased by 33% and 40%, respectively, compared to the control mixture. However, exceeding 0.3% GQDs addition resulted in adverse effect on mechanical properties. This is attributed to the increased porosity caused by the incorporation of GQDs. In addition, the environmental assessment revealed that increasing GQD content reduced embodied CO_2 emissions, with 0.3% GQDs exhibiting the highest eco-strength efficiency. Therefore, incorporating GQDs, particularly at 0.3%, presents a promising strategy for developing eco-friendly construction materials. For future investigations on GQDs, a more comprehensive examination of their properties is warranted to evaluate their potential as suitable materials for industrial applications. Such research could facilitate the development of environmentally friendly materials and contribute to the reduction of CO_2 emissions.

Acknowledgement

This Research is funded by Thailand Science research and Innovation Fund Chulalongkorn University (BCG_FF_68_108_2100_016). The authors gratefully acknowledge CrystalLyte Co., Ltd. for providing the graphene quantum dots.

References

[1] Wu, M., Zhang, Y., Liu, Z., Liu, C., She, W., & Wu, Z. (2024). Experimental study on eco-friendly one-part alkali-activated slag-fly ash-lime composites under CO_2 environment: Reaction mechanism and carbon capture capacity. *Construction and Building Materials*, *421*, 135779.

[2] Han, S. H., Kim, S. M., Jun, Y., Han, T. H., & Kim, J. H. (2024). *Carbon-captured sodium hydroxide solution for sustainable alkali-activated slag. Sustainable Materials and Technologies 40, e00915*.

[3] Hamcumpai, K., Nuaklong, P., Chindasiriphan, P., Jongvivatsakul, P., Tangaramvong, S., Di Sarno, L., & Likitlersuang, S. (2024). High-strength steel fibre-reinforced geopolymer concrete utilising recycled granite waste and rice husk ash. *Construction and Building Materials*, *433*, 136693.

[4] Provis, J. L. (2018). Alkali-activated materials. *Cement and concrete research*, *114*, 40-48.

[5] Wu, W., Li, Y., Du, X., Zhao, H., Kong, J., Wang, L., Chen, M., & Quan, H. (2024). Formulation and characterization of one-part Ca-based alkali-activated slag-steel slag materials. *Construction and Building Materials*, *449*, 138432.

[6] Ankur, N., & Singh, N. (2021). Performance of cement mortars and concretes containing coal bottom ash: A comprehensive review. *Renewable and Sustainable Energy Reviews*, *149*, 111361.

[7] Chindasiriphan, P., Nuaklong, P., Keawsawasvong, S., Thongchom, C., Jirawattanasomkul, T., Jongvivatsakul, P., Tangchirapat, W., & Likitlersuang, S. (2023). Effect of superabsorbent polymer and polypropylene fiber on mechanical performances of alkali-activated high-calcium fly ash mortar under ambient and elevated temperatures. *Journal of Building Engineering*, *71*, 106509.

[8] Nuaklong, P., Hamcumpai, K., Keawsawasvong, S., Pethrung, S., Jongvivatsakul, P., Tangaramvong, S., Pothisiri, T., & Likitlersuang, S. (2023). Strength and post-fire performance of fiber-reinforced alkali-activated fly ash concrete containing granite industry waste. *Construction and Building Materials*, *392*, 131984.

[9] Choeycharoen, P., Sornlar, W., & Wannagon, A. (2022). A sustainable bottom ash-based alkali-activated materials and geopolymers synthesized by using activator solutions

from industrial wastes. *Journal of Building Engineering*, *54*, 104659.

[10] Alsalman, A., Assi, L. N., Kareem, R. S., Carter, K., & Ziehl, P. (2021). Energy and CO_2 emission assessments of alkali-activated concrete and Ordinary Portland Cement concrete: A comparative analysis of different grades of concrete. *Cleaner Environmental Systems*, *3*, 100047.

[11] Duxson, P., Provis, J. L., Lukey, G. C., & Van Deventer, J. S. (2007). The role of inorganic polymer technology in the development of 'green concrete'. *cement and concrete research*, *37*(12), 1590-1597.

[12] Win, T. T., Raengthon, N., & Prasittisopin, L. (2024). Advanced cement composites: Investigating the role of graphene quantum dots in improving thermal and mechanical performance. *Journal of Building Engineering*, *96*, 110556.

[13] Exarchos, D. A., Dalla, P. T., Tragazikis, I. K., Alafogianni, P., Barkoula, N. M., Paipetis, A. S., Dassios, K. G., & Matikas, T. E. (2014). Thermal and electrical behavior of nano-modified cement mortar. In *Smart Sensor Phenomena, Technology, Networks, and Systems Integration 2014* (Vol. 9062, pp. 303-312). SPIE.

[14] Win, T. T., Prasittisopin, L., Nganglumpoon, R., Pinthong, P., Watmanee, S., Tolek, W., & Panpranot, J. (2024). Innovative GQDs and supra-GQDs assemblies for developing high strength and conductive cement composites. *Construction and Building Materials*, *421*, 135693

[15] Raj, A., Yamkasikorn, P., Wangtawesap, R., Win, T. T., Ngamkhanong, C., Jongvivatsakul, P., Prasittisopin, L., Panpranot, J., & Kaewunruen, S. (2024). Effect of Graphene Quantum Dots (GQDs) on the mechanical, dynamic, and durability properties of concrete. *Construction and Building Materials*, *441*, 137597.

[16] ASTM C618, (2005). Standard specification for coal fly ash and raw or calcined natural pozzolan for use as a mineral admixture in concrete. ASTM C618-05. Annual Book of ASTM Standards, 4(2).

[17] ASTM C33, (2003). Standard specification for concrete aggregates. ASTM C33-03. Annual Book of ASTM Standards, 4(2).

[18] ASTM C1437, (2015). Standard Test Method for Flow of Hydraulic Cement Mortar. ASTM C1437-15. Annual Book of ASTM Standards, 4(2).

[19] ASTM C109, (2016). Standard Test Method for Compressive Strength of Hydraulic Cement Mortars (Using 2-in. or [50-mm] Cube Specimens). ASTM C109/C109M-16a. Annual Book of ASTM Standards, 4(2).

[20] ASTM C348, (2002). Standard Test Method for Flexural Strength of Hydraulic Cement Mortars. ASTM C348-02. Annual Book of ASTM Standards, 4(2).

[21] ASTM C642, (2013). Standard Test Method for Density, Absorption, and Voids in Hardened Concrete. ASTM C642-13. Annual Book of ASTM Standards, 4(2).

[22] Haruna, S., Jongvivatsakul, P., Hamcumpai, K., Iqbal, H. W., Nuaklong, P., Likitlersuang, S., & Iwanami, M. (2024). Multiscale investigation of the impact of recycled plastic aggregate as a fine aggregate replacement on one-part alkali-activated mortar performance. *Journal of Building Engineering*, *86*, 108768.

[23] Zhang, S. L., Qi, X. Q., Guo, S. Y., Ren, J., Chen, J. Z., Chi, B., & Wang, X. C. (2021). Effect of a novel hybrid TiO2-graphene composite on enhancing mechanical and durability characteristics of alkali-activated slag mortar. *Construction and Building Materials*, *275*, 122154.

[24] Mohammed, A., Sanjayan, J. G., Duan, W. H., & Nazari, A. (2015). Incorporating graphene oxide in cement composites: A study of transport properties. *Construction and Building Materials*, *84*, 341-347.

[25] Indukuri, C. S. R., & Nerella, R. (2021). Enhanced transport properties of graphene oxide based cement composite material. *Journal of Building Engineering*, *37*, 102174.

[26] Yan, Y., Gong, J., Chen, J., Zeng, Z., Huang, W., Pu, K., Liu, J., & Chen, P. (2019). Recent advances on graphene quantum dots: from chemistry and physics to applications. *Advanced materials*, *31*(21), 1808283.